Supporting Information

cmc-Measurements: Determination of Interaction Parameter

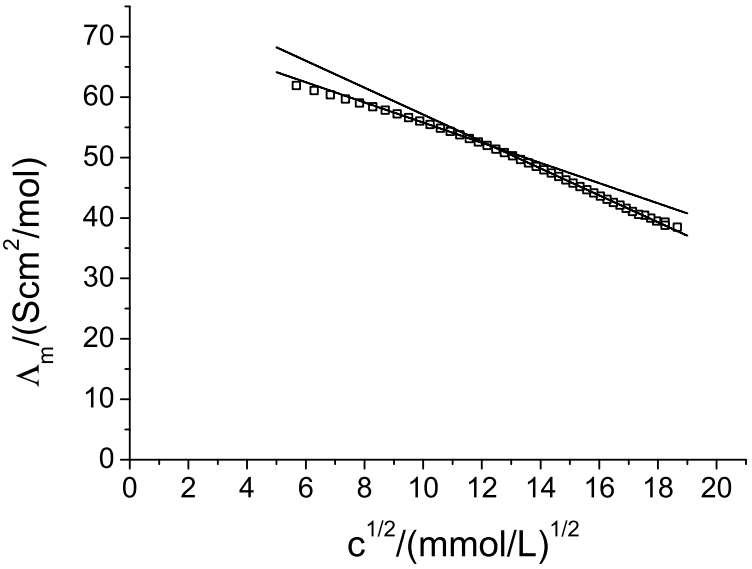

Figure S1: Determination of the cmc by conductivity measurements on the system TDMAO-$C_5F_{11}CO_2Li$ at $\alpha(\text{TDMAO}) = 0$ □

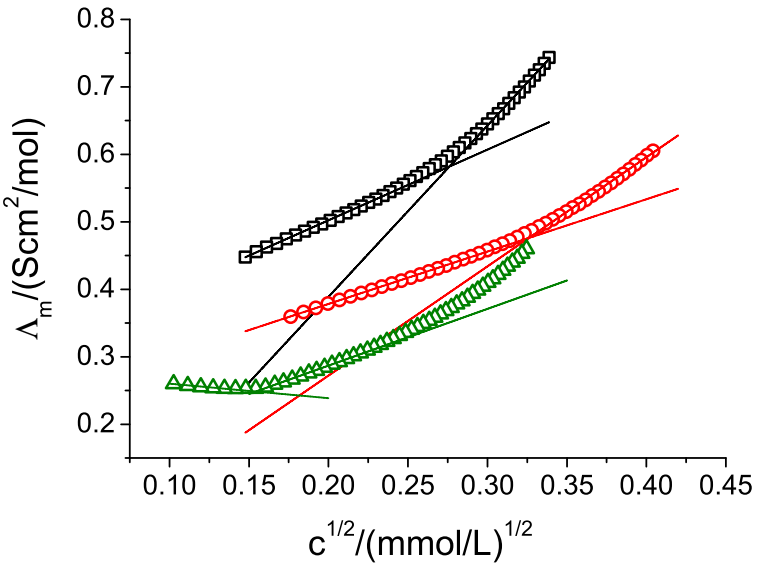

Figure S2: Determination of the cmc by conductivity measurements on the system TDMAO-$C_5F_{11}CO_2Li$ at α(TDMAO) = 0.1 □, α(TDMAO) = 0.3 ◯, and α(TDMAO) = 0.5 △

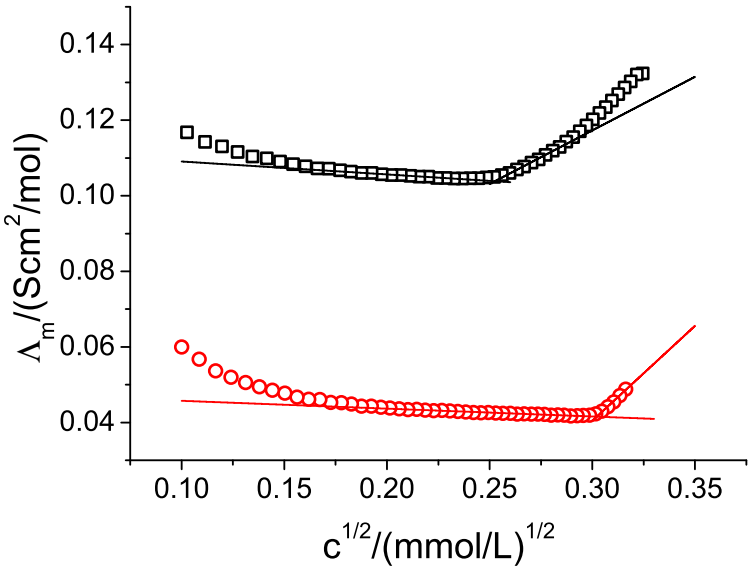

Figure S3: Determination of the cmc by conductivity measurements on the system TDMAO-$C_5F_{11}CO_2Li$ at α(TDMAO) = 0.7 □ and α(TDMAO) = 0.9 ◯

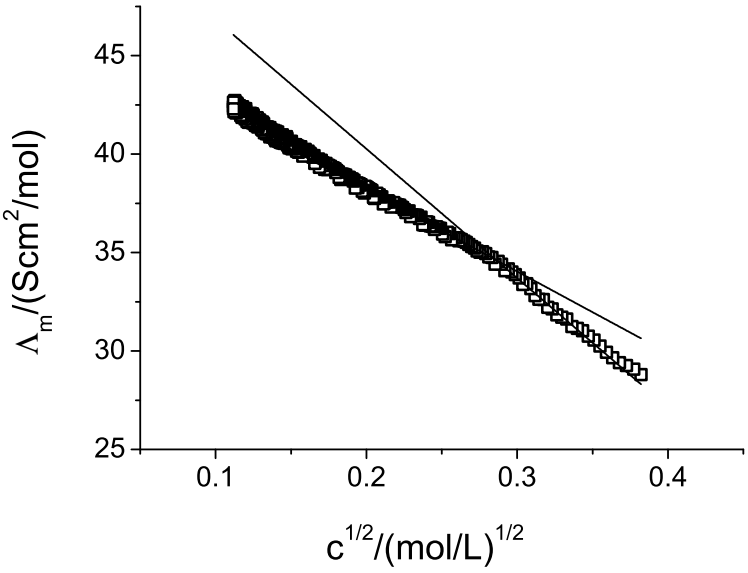

Figure S4: Determination of the cmc by conductivity measurements on the system TDMAO-$C_6F_{13}CO_2Li$ at α(TDMAO) = 0 □

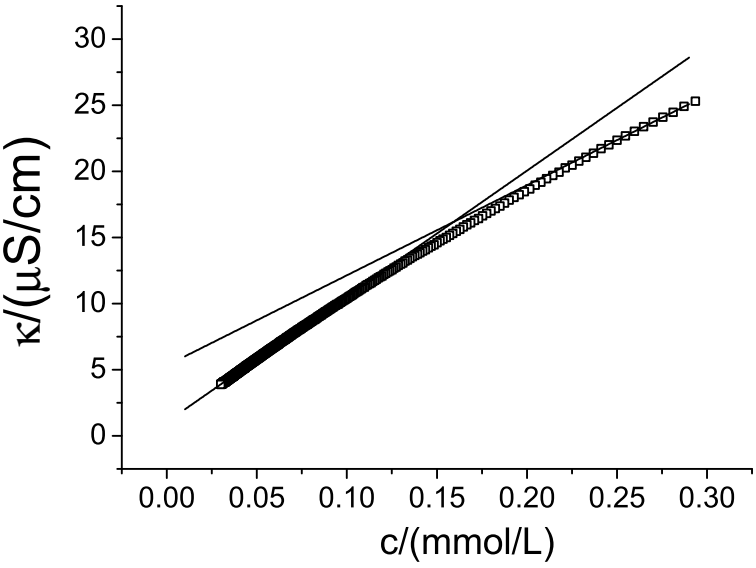

Figure S5: Determination of the cmc by conductivity measurements on the system TDMAO-$C_6F_{13}CO_2Li$ at α(TDMAO) = 0.1 □

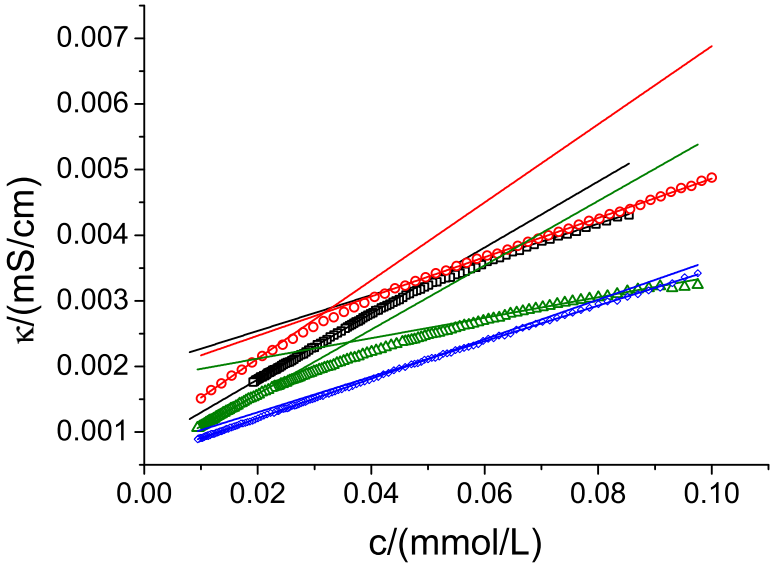

Figure S6: Determination of the cmc by conductivity measurements on the system TDMAO-$C_6F_{13}CO_2Li$ at α(TDMAO) = 0.3 □, α(TDMAO) = 0.4 ◯, α(TDMAO) = 0.5 △, and α(TDMAO) = 0.7 ◊

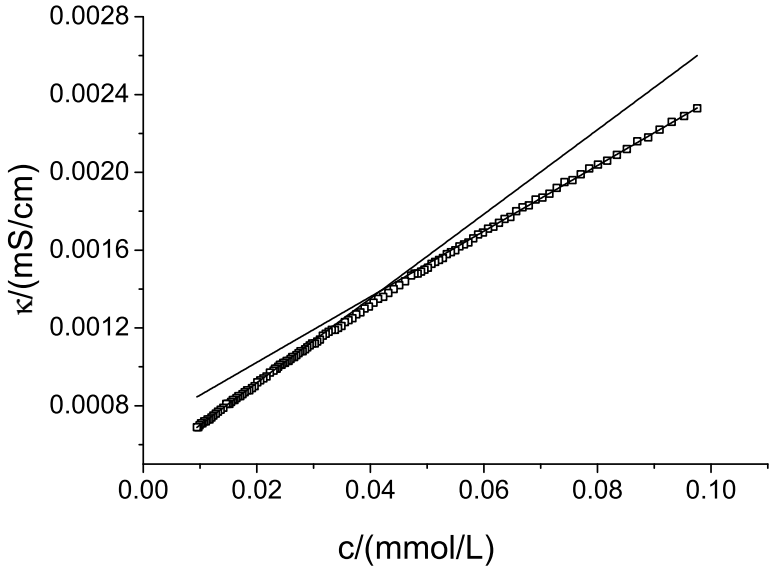

Figure S7: Determination of the cmc by conductivity measurements on the system TDMAO-$C_6F_{13}CO_2Li$ at α(TDMAO) = 0.9 □

Phase Behaviour

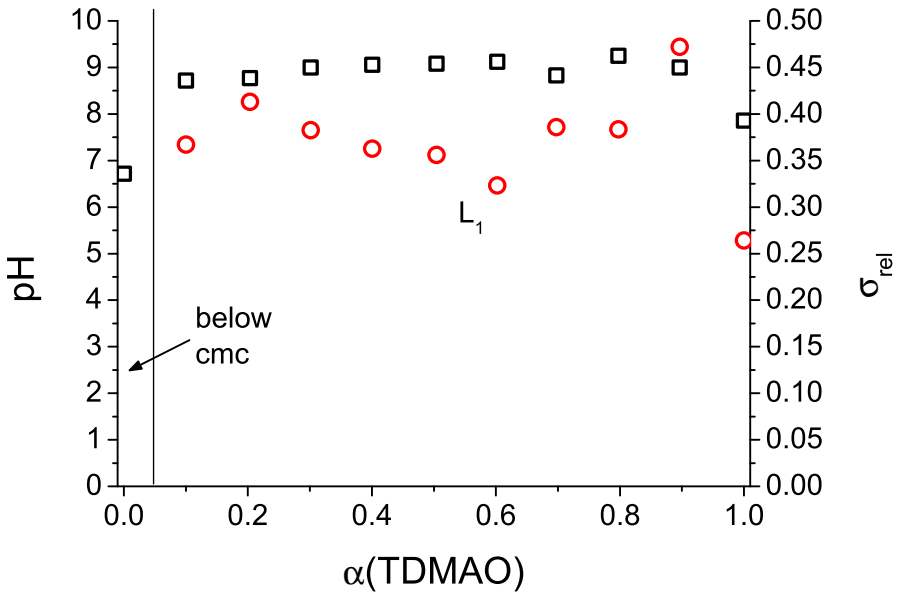

Figure S8: pH □ and polydispersity index (σ_{rel}) from DLS ◯ as a function of the molar ratio of the TDMAO (α(TDMAO)) in the mixture TDMAO/$C_5F_{11}CO_2Li$ at $50mM$ total concentration ($T = 25°C$)

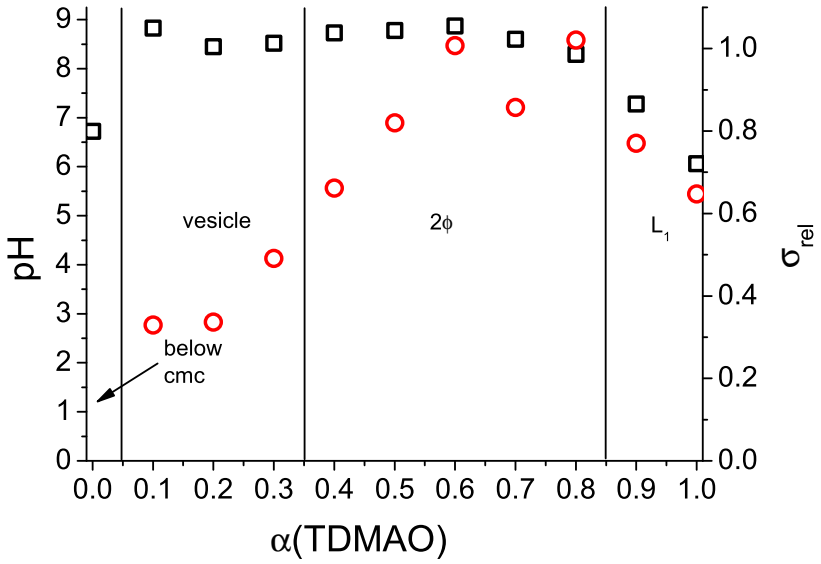

Figure S9: pH □ and polydispersity index (σ_{rel}) determined by DLS measurements ◯ of the system TDMAO/HCl/$C_5F_{11}CO_2Li$ at $50mM$ total concentration ($T = 25°C$) as a function of the molar ratio of the TDMAO (α(TDMAO))

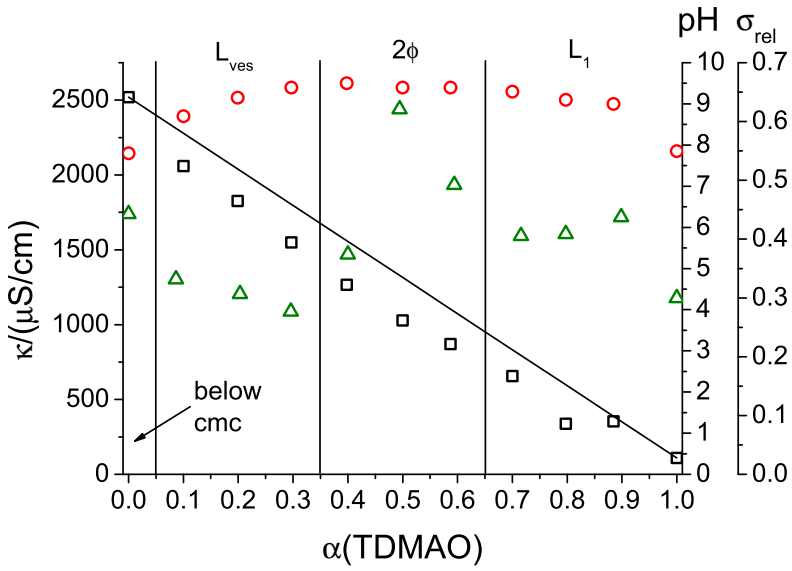

Figure S10: Phase behaviour and corresponding conductivity (κ) □, pH ◯, and polydispersity index △ determined from cumulant analysis of the system TDMAO/$C_6F_{13}CO_2Li$ at a total concentration of $50mM$ ($T = 25°C$) as a function of the molar ratio of the TDMAO (α(TDMAO))

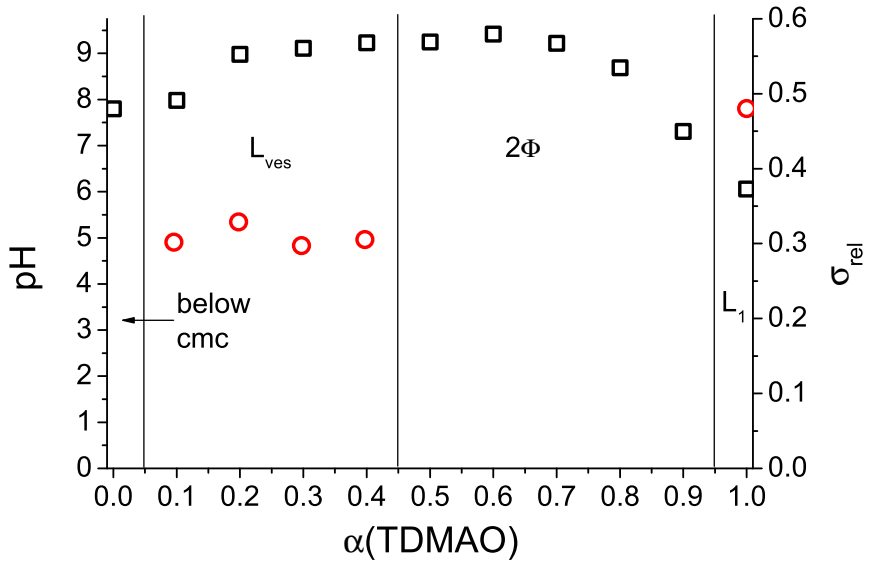

Figure S11: pH □ and polydispersity index (σ_{rel}) determined by DLS measurements ◯ of the system TDMAO-$C_6F_{13}CO_2Li$-HCl with $c(\mathrm{HCl})/c(\mathrm{TDMAO}) = 0.1$ at a constant total concentration of 50 mM ($T = 25°C$) as a function of the molar ratio of the TDMAO (α(TDMAO))

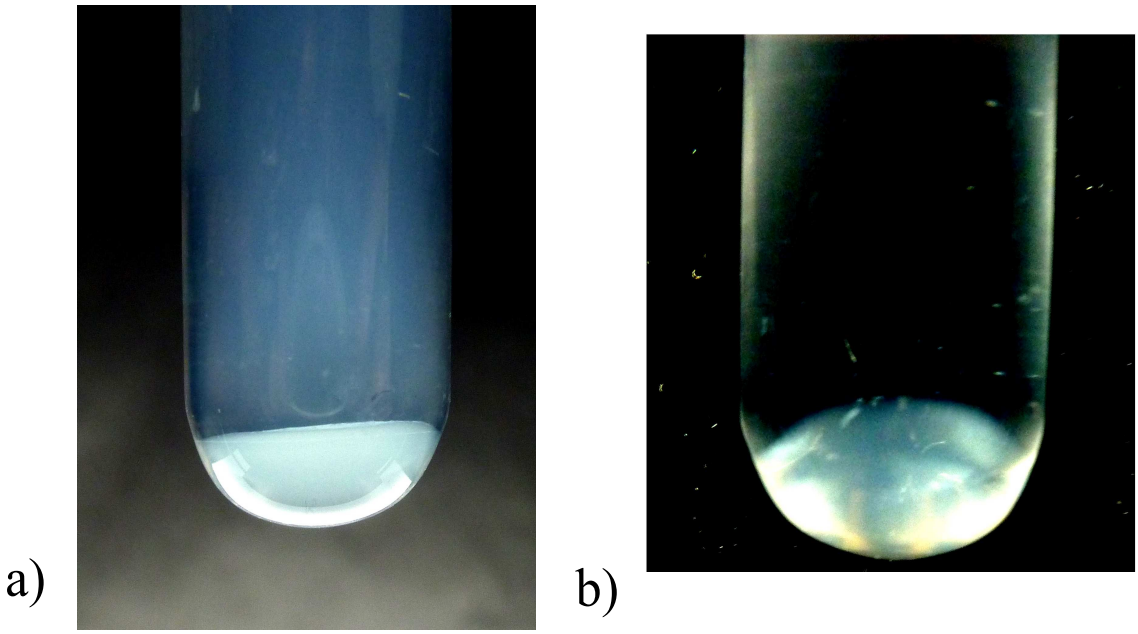

Figure S12: Photo of a mixture of TDMAO-$C_6F_{13}CO_2Li$ with $50mM$ and $\alpha(\mathrm{TDMAO}) = 0.5$, sample is between polarization filters in photo b)

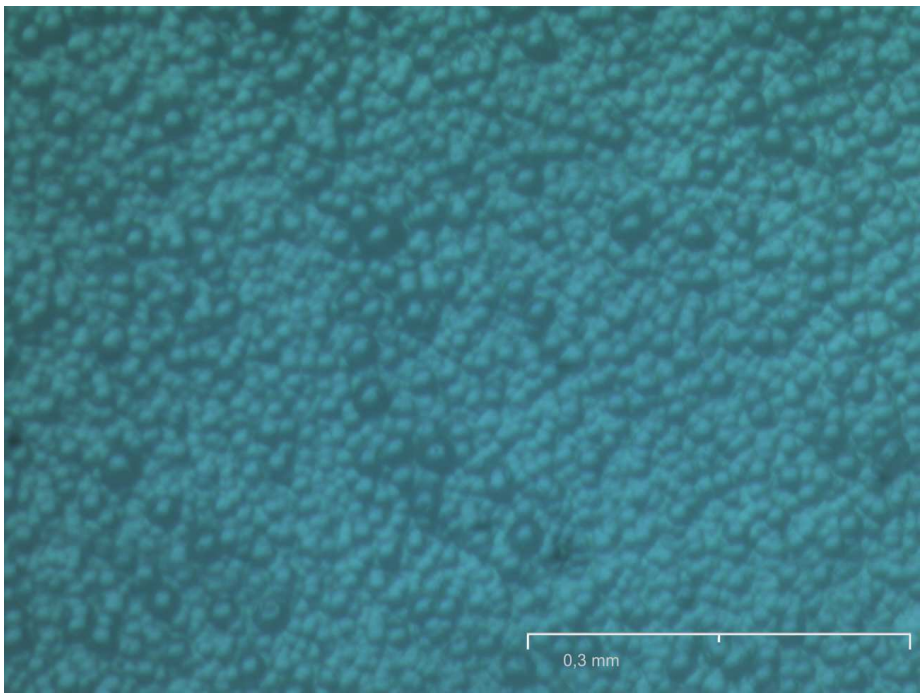

Figure S13: Photo of a mixture of TDMAO-$C_6F_{13}CO_2Li$ with $50mM$ and α(TDMAO) = 0.5 under a microscope with a tenfold magnification

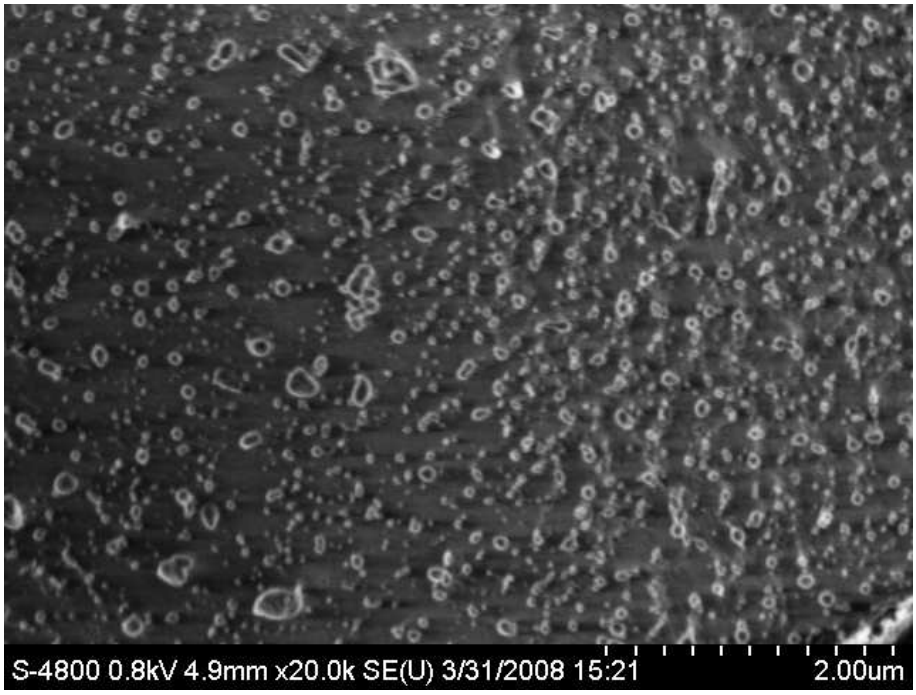

Figure S14: Cryo-SEM micrograph of a mixture of TDMAO-$C_6F_{13}CO_2Li$ with $50mM$ and α(TDMAO) = 0.2; mostly vesicles with a radius of $50nm$ are formed beside large objects of radii up to $300nm$

DLS-measurements

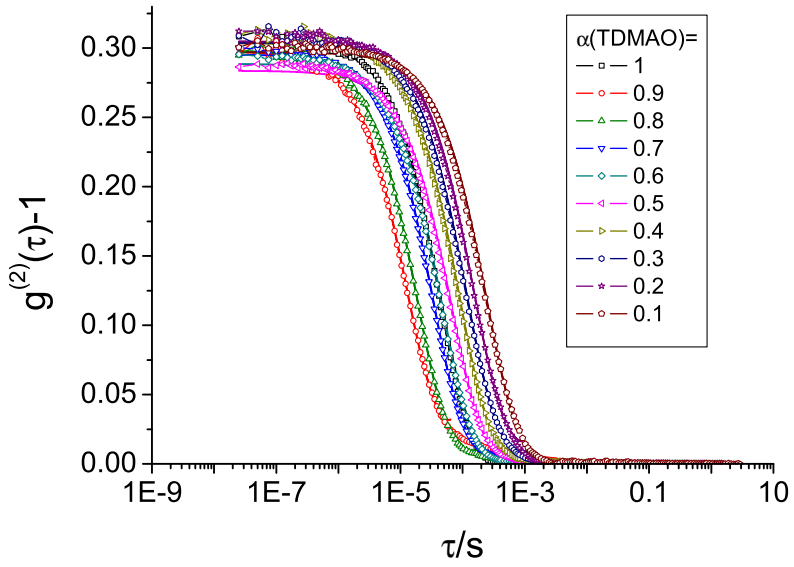

Figure S15: Normalised intensity autocorrelation functions of the DLS measurements (symbols) and cumulant analysis (lines) on the system TDMAO-$C_5F_{11}CO_2Li$ with a total surfactant concentration of $50mM$ at a temperature of $25°C$

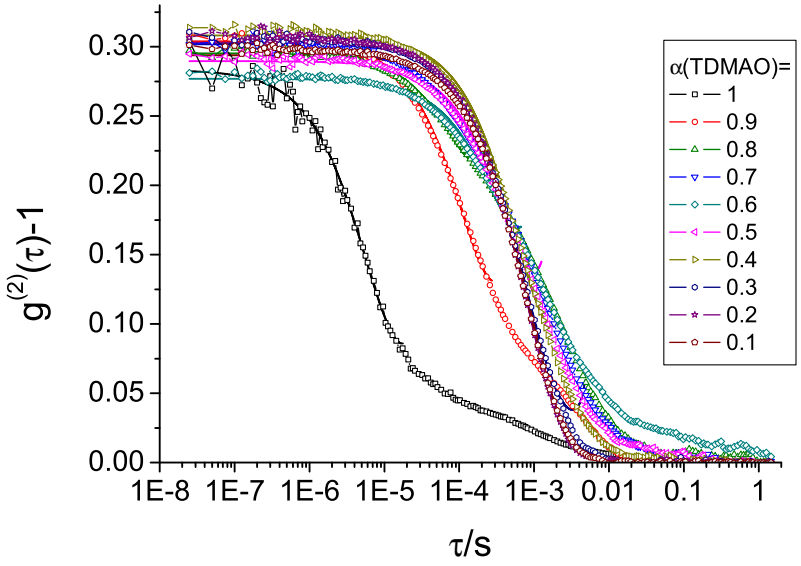

Figure S16: Normalised intensity autocorrelation functions of the DLS measurements (symbols) and cumulant analysis (lines) on the system TDMAO-$C_5F_{11}CO_2Li$-HCl with a total surfactant concentration of $50mM$ and a HCl-concentration of $c(\mathrm{HCl}) = 0.1 \cdot c(\mathrm{TDMAO})$ at a temperature of $25°C$

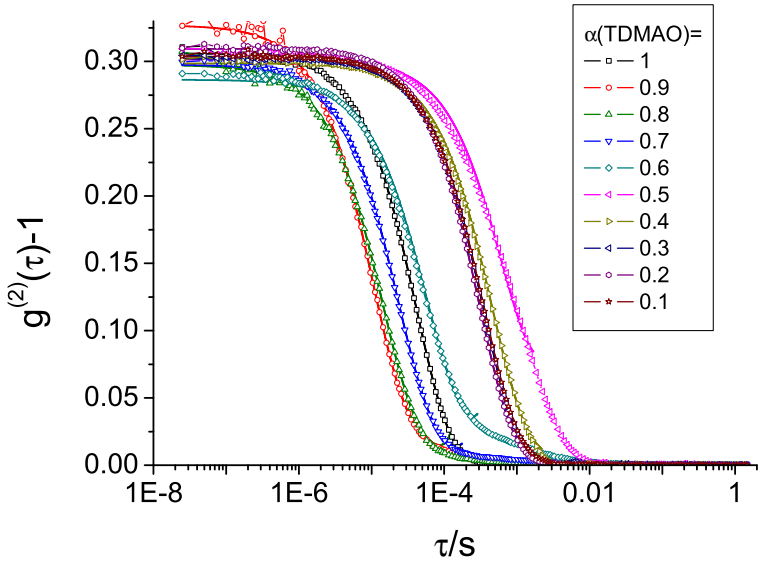

Figure S17: Normalised intensity autocorrelation functions of the DLS measurements (symbols) and cumulant analysis (lines) on the system TDMAO-$C_6F_{13}CO_2Li$ (0.59:0.41) with a total surfactant concentration of $50mM$ at a temperature of $25°C$

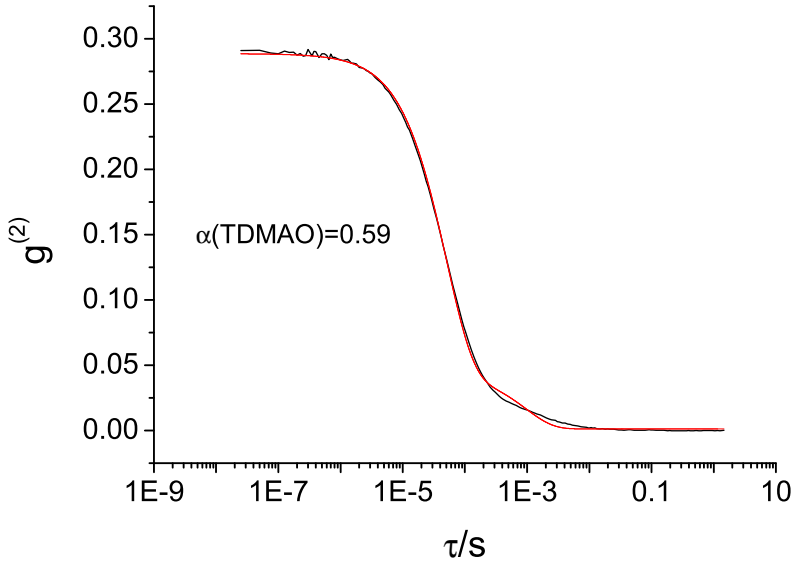

Figure S18: Normalised intensity autocorrelation functions of the DLS measurement (symbols) and bi-exponential fit (lines) on the system TDMAO-$C_6F_{13}CO_2Li$ (0.59:0.41) with a total surfactant concentration of $50mM$ at a temperature of $25°C$

α(TDMAO)	$R_{h,cumu.}/nm$	PDI	$\eta/mPas$	$R_{h1,biexp.}/nm$	$R_{h2,biexp.}/nm$	α(TDMAO)	$R_{cond.}/nm$
1.00	7	0.3	1.16			1.00	
0.90	2	0.44	3.54			0.88	
0.80	2	0.41	2.84			0.80	
0.72	4	0.41	13.78			0.70	
0.59	10	0.49	23.55	9	164	0.59	91
0.49	129	0.62	15.31			0.50	97
0.40	78	0.37	10.67			0.40	87
0.30	60	0.28	3.27			0.30	67
0.20	52	0.31	1.44			0.20	52
0.09	59	0.33	0.98			0.10	50
0.00			0.96			0.00	

Table S1: hydrodynamic Radii R_h determined from cumulant analysis and from biexponentiell fits, polydispersity index PDI determined from cumulant analysis, vesicle radius R determined from conductivity measurements and viscosity η as a function of the molar fraction a of the TDMAO in the system TDMAO-$C_6F_{13}CO_2Li$ ($T = 25°C$)

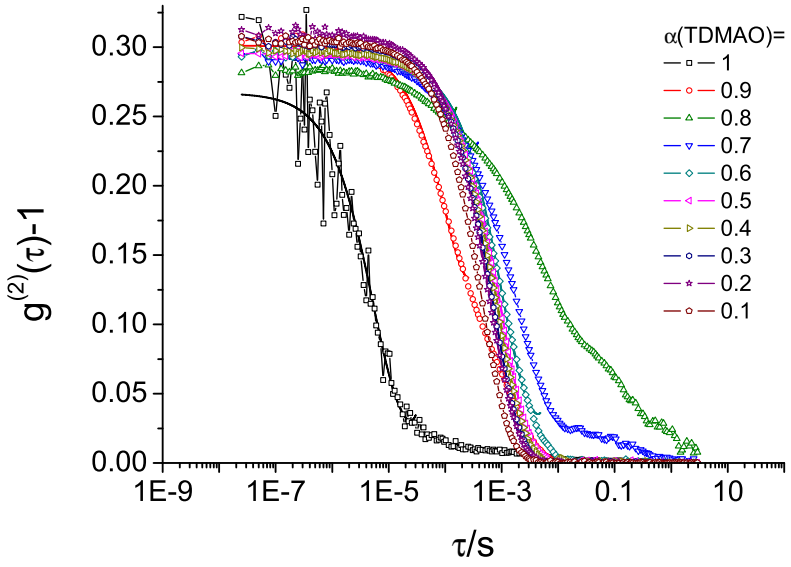

Figure S19: Normalised intensity autocorrelation functions of the DLS measurements and cumulant analysis on the system TDMAO-$C_6F_{13}CO_2Li$-HCl with a total surfactant concentration of $50mM$ and a HCl-concentration of $c(\mathrm{HCl}) = 0.1 \cdot c(\mathrm{TDMAO})$ at a temperature of $25°C$

Small Angle Neutron Scattering (SANS)

The scattering length density of the mixed material $SLD_{particle}$ is a volume fraction (ϕ_A and ϕ_B) weighted sum of the scattering length densities SLD_A and SLD_B of the components A and B. The scattering length density contrast ΔSLD is the difference between the scattering length density of the particles $SLD_{particle}$ and the medium $SLD_{\mathrm{D_2O}}$.

$$\Delta SLD = SLD_{\mathrm{D_2O}} - (\phi_A SLD_A + \phi_B SLD_B) \tag{S1}$$

The scattering intensity $I_{cyl}(q)$ for monodisperse cylinders or discs with the form factor $P_{cylinder}(q)$, the length L, the radius R_{cyl}, the volume fraction of the scattering material ϕ_{amph} and the scattering contrast compared to the surrounding medium ΔSLD is given by:

$$P_{cyl}(q, R_{cyl}, L) = 4 \int_0^{\pi/2} \frac{\sin\left(\frac{qL}{2}\cos(\theta)\right)}{\frac{qL}{2}\cos(\theta)} \cdot \frac{J_1\left(qR_{cyl}\sin(\theta)\right)}{\left(qR_{cyl}\sin(\theta)\right)^2} d\theta \tag{S2}$$

$$I_{cyl}(q, R_{cyl}, L) = \frac{\phi_{amph}}{V_{cyl}(R_{cyl}, L)} \cdot \Delta SLD^2 \cdot V_{cyl}^2(R_{cyl}, L) \cdot P_{cyl}^2(q, R_{cyl}, L) \tag{S3}$$

$$\text{with} \quad V_{cyl}(R_{cyl}, L) = \pi R_{cyl} L$$

where J_1 is the Bessel function of the first order.
That leads to the following scattering intensity for the micelles with a log-normal distributed length L for cylindrical micelles:

$$I_{cyl}(q, R_{cyl}, L_0, \sigma) = \phi_{amph} \cdot \frac{\int_0^\infty LogNorm(L, L_0, \sigma) \cdot \Delta SLD^2 \cdot V_{cyl}^2(R_{cyl}, L) \cdot P_{cyl}^2(q, R_{cyl}, L) dL}{\int_0^\infty LogNorm(L, L_0, \sigma) \cdot V_{cyl}(R_{cyl}, L) dL} \tag{S4}$$

The log-normal distribution of a parameter t is given as:

$$LogNorm(t, \mu_L, \sigma_L) = \frac{1}{t\sqrt{2\pi}\sigma_L} \exp\left(\frac{-(\ln(t) - \mu_L)^2}{2\sigma_L}\right) \tag{S5}$$

The parameters μ_L and σ_L are linked to the mean μ of the distribution and the standard deviation σ which is identical to the polydispersity index PDI and throughout the text named polydispersity:

$$\sigma_L = \sqrt{\ln(\sigma + 1)} \tag{S6}$$

$$\mu_L = \ln(\mu) - \frac{\sigma_L^2}{2} \tag{S7}$$

For polydisperse vesicles (spherical shells) with a log-normal distributed intermediate radius R, a mean radius of R_0 and a relative standard deviation σ the scattering intensity is given by:

$$P_{vesicle}(q, R) = \Delta SLD(f(q, R_{out}(R)) - f(q, R_{in}(R))) \tag{S8}$$

$$\text{with} \quad f(q, R) = 4\pi R^3 \cdot \frac{\sin(qR) - qR\cos(qR)}{(qR)^3}$$

$$I_{vesicle}(q, R_0, \sigma) = \phi_{amph} \cdot \frac{\int_0^\infty LogNorm(R, R_0, \sigma) P_{vesicle}^2(q, R) dR}{\int_0^\infty LogNorm(R, R_0, \sigma) \cdot V_{shell}(R) dR} \tag{S9}$$

$$\text{with} \quad V_{shell}(R) = \frac{4\pi}{3}\left(R_{out}^3(R) - R_{in}^3(R)\right)$$

with $R_{out} = R + d/2$ and $R_{in} = R - d/2$.
The RPA structure factor for electrostatic repulsion $S(q)$ is described by eqn (S10) with the effective radius R_{eff} and the surface potential ζ as fit parameters and the inverse Debye screening length k_D, the Boltzmann constant k_B, the temperature T and the dielectric constant of the medium, here water, ϵ as constant parameters.

$$S(q) = \frac{1}{1 - nC(q)} \tag{S10}$$

$$nC_0(q) = \left[A(\sin(x) - x\cos(x)) + B\left[\left(\frac{2}{x^2} - 1\right)x\cos(x) + 2\sin(x) - \frac{2}{x}\right]\right.$$
$$\left. - \frac{\phi_{eff}A}{2}\left[\frac{24}{x^3} + 4\left(1 - \frac{6}{x^2}\right)\sin(x) - \left(1 - \frac{12}{x^2} + \frac{24}{x^4}\right)x\cos(x)\right]\right]x^{-3} \tag{S11}$$

with $x = 2qR_{eff}$

$$nC(q) = nC_0(q) - 48\frac{\phi_{eff}\pi\epsilon R_{eff}\zeta^2(x\cos(x) + 2k_D R_{eff}\sin(x))}{k_B T x(x^2 + 4k_D^2 R_{eff}^2)} \tag{S12}$$

with the factors

$$A = -24\phi_{eff}\frac{(1 + 2\phi_{eff})^2}{(1 - \phi_{eff})^4} \quad \text{and} \quad B = 36\phi_{eff}^2\frac{(2 + \phi_{eff})^2}{(1 - \phi_{eff})^4}$$

The effective volume fraction of the particles ϕ_{eff} is calculated from the particle number density N_V which is determined from the form factor.

$$\phi_{eff} = N_V\pi\frac{4}{3}R_{eff}^3 \tag{S13}$$

The particle number density N_V is described for the form factor as well as for the structure factor by eqn (S14).

$$N_V = \frac{\phi_{amph}}{V_{aggregate}} \tag{S14}$$

In the case of polydisperse particles with a normalised distribution *dist* of a parameter t the particle number density is described by eqn (S15).

$$N_V = \frac{\phi_{amph}}{\int_0^\infty dist(t, t_0, \sigma) \cdot V_{aggregate}(t)dt} \tag{S15}$$

The volume of the aggregates $V_{aggregate}$ being the volume of scattering material in a single aggregate. For vesicles that would be only the vesicle shell. The volume fraction of the scattering material ϕ_{amph} is calculated from the total concentration of amphiphile c_{tot} and the molar mass M_i and the density ρ_i of the amphiphilic components i:

$$\phi_{amph} = c_{tot} \cdot \sum_i \left(\frac{M_i}{\rho_i}\right) \tag{S16}$$

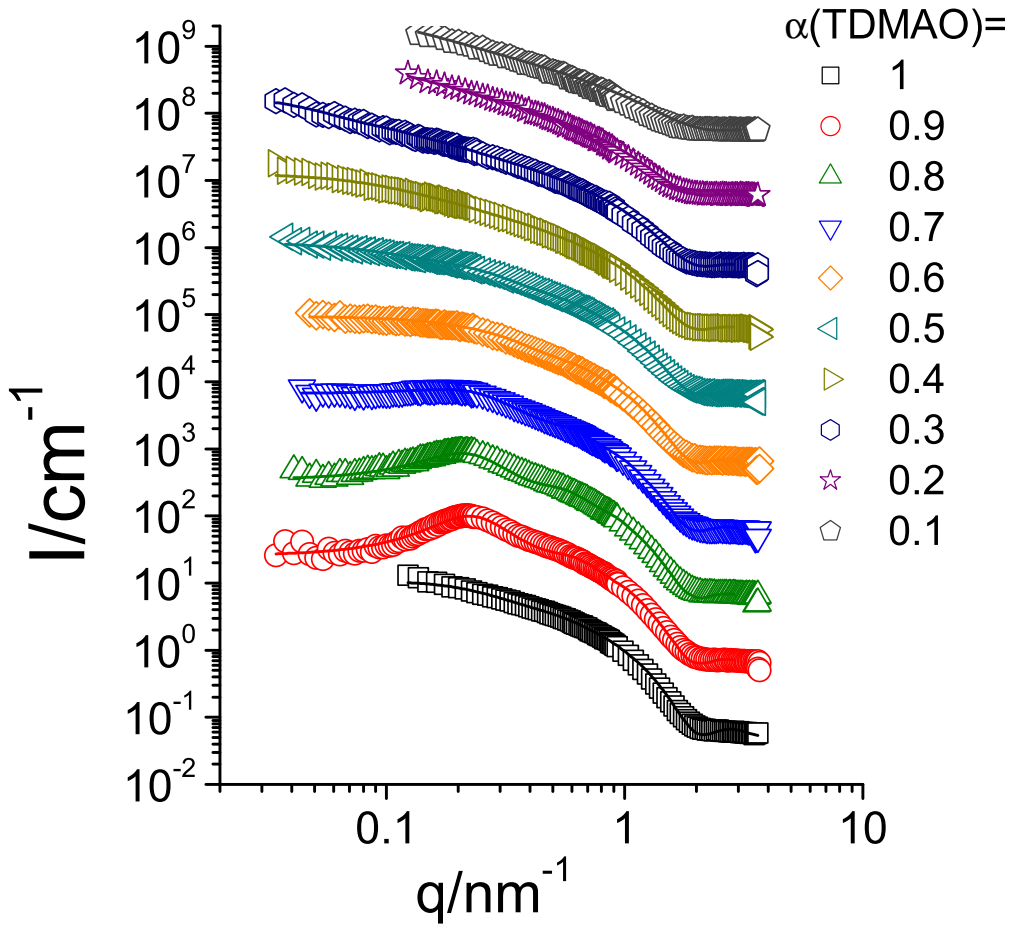

Figure S20: Small Angle Neutron Scattering (SANS) measurements of mixtures of TDMAO-$C_5F_{11}CO_2Li$, (50 mM, 25°C, at α(TDMAO) = 0 no measurement is shown since here one is below the *cmc*, data are multiplied by multiples of 10 for clarification)

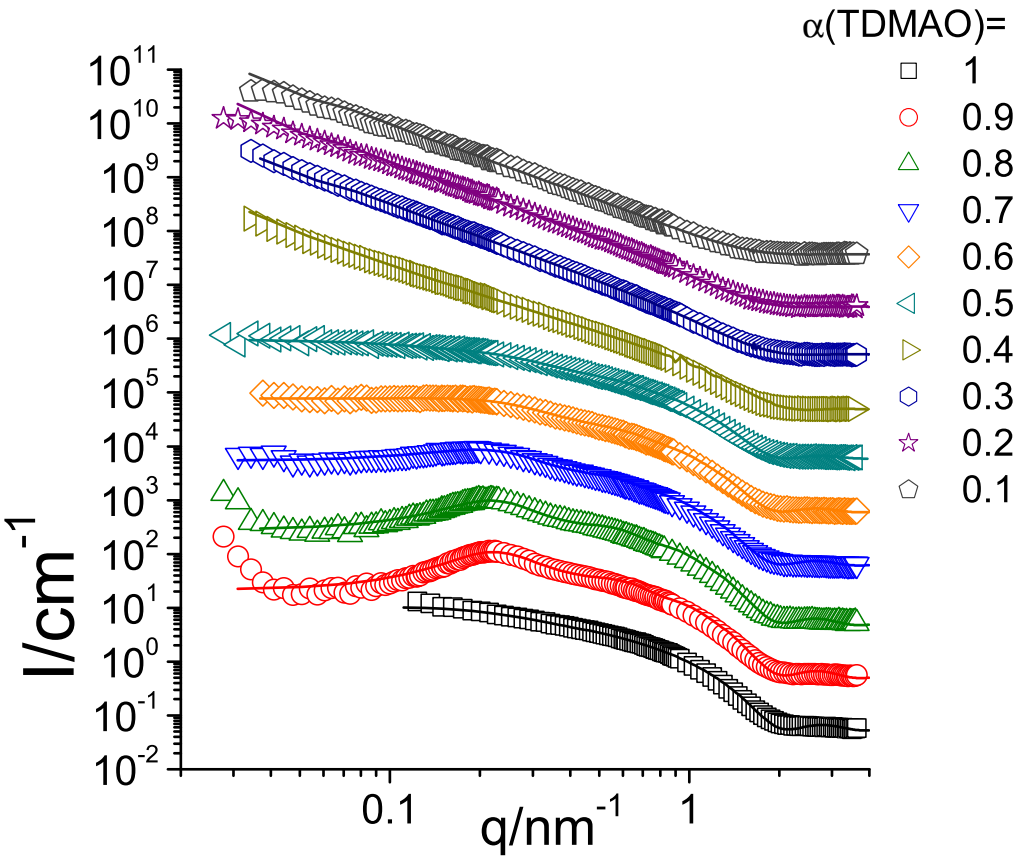

Figure S21: Small Angle Neutron Scattering (SANS) measurements of mixtures of TDMAO-$C_6F_{13}CO_2Li$, (50 mM, 25°C, at α(TDMAO) = 0 no measurement is shown since here one is below the *cmc*, data are multiplied by multiples of 10 for clarification)

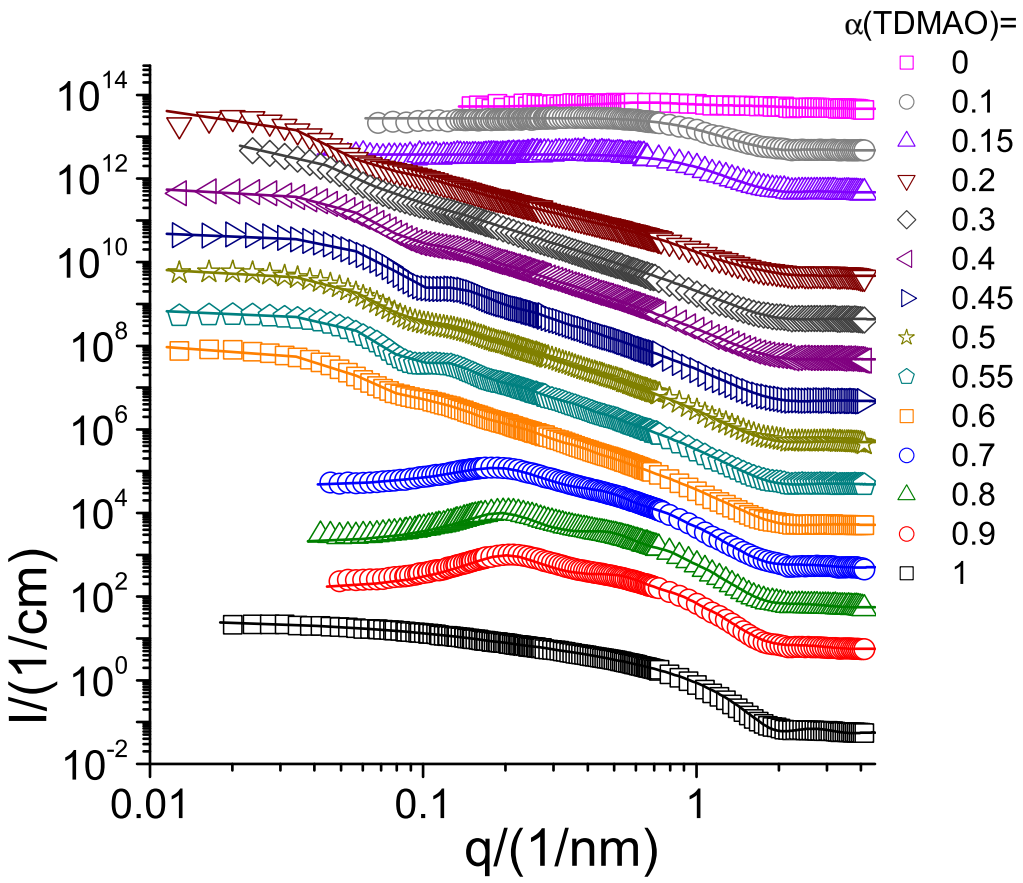

Figure S22: Small Angle Neutron Scattering (SANS) measurements of mixtures of TDMAO-$C_7F_{15}CO_2Li$, (50 mM, 25°C, at α(TDMAO) = 0 no measurement is shown since here one is below the *cmc*, data are multiplied by multiples of 10 for clarification)

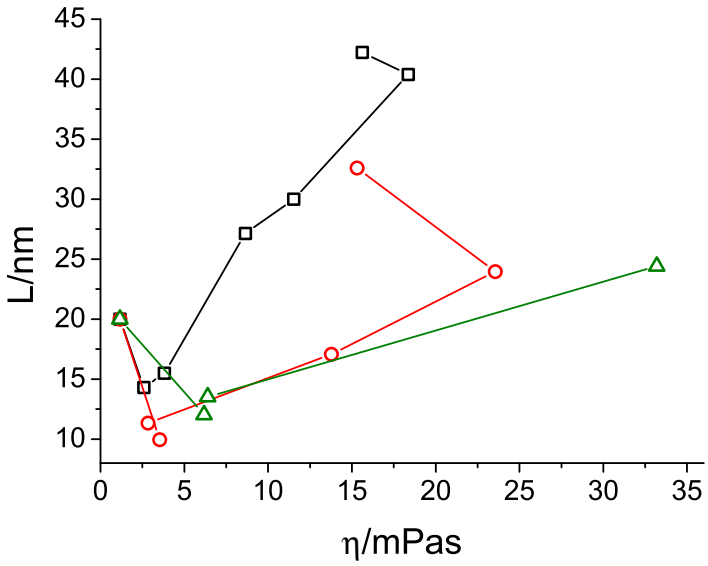

Figure S23: Dependency of the length (L) of the micelles derived from SANS-measurements on the viscosity (η) of the sample in the system TDMAO-$C_nF_{2n+1}CO_2Li$ with a constant total concentration of $50mM$ at $25°C$; n=5 □, n=6 ◯, n=7 △